J. Membrane Biol. 163, 37–46 (1998)

The Journal of
Membrane
Biology

Vestibular Dark Cells Contain an H^+/Monocarboxylate$^-$ Cotransporter in Their Apical and Basolateral Membrane

M. Shimozono[1], **J. Liu**[1], **M.A. Scofield**[2], **P. Wangemann**[1]

[1]Cell Physiology Laboratory, Boys Town National Research Hospital, Omaha, NE 68131, USA
[2]Molecular Pharmacology Laboratory, Creighton University, Omaha, NE 68178, USA

Received: 5 June 1997/Revised: 30 January 1998

Abstract. The transport of lactate and pyruvate across membranes of vestibular dark cells (VDC) may be important under aerobic, ischemic or hypoxic conditions. This study addresses the questions whether VDC from the gerbil contain an H^+/monocarboxylate$^-$ cotransporter (MCT) and in which membrane, apical or basolateral, MCT is located. Uptake of monocarboxylates into VDC was monitored in functional studies by measuring the cytosolic pH (pH_i) and by measuring the pH-sensitive equivalent short circuit current (I_{sc}). Subtypes of the functionally identified MCT which are present in vestibular labyrinth tissues were identified as transcripts by cloning and sequencing of reverse-transcriptase polymerase chain reaction (RT-PCR) products. Monocarboxylates but not dicarboxylates induced a transient acidification of pH_i which was inhibited by 5 mM α-cyano-4-hydroxycinnamate (CHC) but not by 1 μM DIDS or 500 μM pCMBS. The initial rate of acidification induced by monocarboxylates was dose-dependent in the range between 1 and 20 mM. K_m values were for pyruvate 1.3, acetate 3.7, L-lactate 3.8 and D-lactate 7.3 mM. Both apical and basolateral application of monocarboxylates caused a transient increase of I_{sc} which was sensitive to 5 mM CHC. RT-PCR revealed the presence of transcripts for the MCT subtypes MCT1 and MCT2. The identity of transcripts was confirmed by sequence analysis. These observations suggest that VDC contain an MCT in their apical and basolateral membrane and that the vestibular labyrinth contains transcripts for the subtypes MCT1 and MCT2.

Key words: H^+/monocarboxylate$^-$ cotransporter — BCECF — Vestibular labyrinth — RT-PCR

Correspondence to: P. Wangemann

Introduction

Vestibular dark cells (VDC) transport K^+ from perilymph to endolymph at a high rate. K^+ is taken up from the basolateral side via the $Na^+/Cl^-/K^+$ cotransporter and the Na,K-ATPase and released across the apical membrane via the I_{sK} channel (Wangemann, 1995). The Na,K-ATPase requires ATP which is generated by aerobic glycolysis. Substrates for glycolysis include glucose as well as pyruvate and lactate. The transport of pyruvate, lactate and other monocarboxylates across plasma membranes of metabolically active cells such as VDC may be important under aerobic conditions as well as under ischemic and hypoxic conditions. To our knowledge, no mechanism for the transport of glycolytic substrate has so far been identified in VDC.

Many mammalian cells are able to transport monocarboxylates across their plasma membranes (Poole & Halestrap, 1993). Uptake of monocarboxylates can be monitored by measuring the cytosolic pH (pH_i) since monocarboxylates are weak acids (Carpenter & Halestrap, 1994; Wang, Levi & Halestrap, 1994). In general, three pathways for monocarboxylate transport have been described: (i) transport via H^+/monocarboxylate$^-$ cotransporters (MCT); (ii) exchange with inorganic anions via anion exchange proteins and (iii) free diffusion of the undissociated acid. These three pathways can be distinguished by their properties. MCT distinguish between the stereo-isomers of lactate, transport monocarboxylates but not dicarboxylates and are inhibited by α-cyano-4-hydroxycinnamate (CHC) (Poole & Halestrap, 1993). Anion exchange proteins catalyzes the exchange of anions such as Cl^-, HCO_3^-, monocarboxylates and dicarboxylates. Anion exchange proteins do not distinguish between D- and L-lactate and are selectively inhibited by low concentrations of 4,4′-diisothiocyanatostilbene-2,2′-disulfonic acid (DIDS) which do not affect MCT (Deu-

ticke, Rickert & Beyer, 1978; Poole & Halestrap, 1993). Both MCT and anion exchange proteins are sensitive to CHC (Halestrap, 1976; Poole & Halestrap, 1993), whereas free diffusion of the undissociated acid would not be expected to be sensitive to inhibitors.

MCT have recently been characterized at the molecular level. Three distinct isoforms, MCT1, MCT2 and MCT3, have so far been cloned and sequenced. MCT1 had first been cloned from Chinese hamster ovary cells (Garcia et al., 1994*b*). Other MCT1 sequences known include those obtained from a human genomic library (Garcia et al., 1994*a*), rat skeletal muscle (Jackson, Price & Halestrap, 1995) and mouse Ehrlich Lettré tumor cells (Carpenter, Poole & Halestrap, 1996). MCT2 has been cloned from Syrian hamster liver (Garcia et al., 1995) and rat testis (Jackson et al., 1997) and MCT3 has recently been cloned from the chick retinal pigment epithelium (Yoon et al., 1997).

Kinetic analyses of MCT1 and MCT2 have revealed only small differences in the substrate selectivity and inhibitor sensitivity (Garcia et al., 1995). These small differences may be physiologically relevant, consistent with the observation of striking differences in the tissue distribution of MCT1 and MCT2 (Garcia et al., 1995, Jackson et al., 1997). These differences, however, may be too small to provide a means for an unambiguous experimental discrimination between MCT1 and MCT2. A more substantial difference between MCT1 and MCT2, the differential sensitivity to p-chloromercuribenzenesulfonic acid (pCMBS), was observed when the isoforms were expressed in Sf9 insect cells (Garcia et al., 1995). MCT1 was found to be sensitive to pCMBS. Consistent with the assumption that MCT in the insect cell expression system is representative of MCT in a native mammalian cell environment is the findings that rat, mouse and human MCT1 are sensitive to pCMBS when studied in native mammalian cell environments such as erythrocytes, Ehrlich Lettré tumor cells and liver cells (Deuticke et al., 1978; Carpenter & Halestrap, 1994; Edlund & Halestrap, 1988; Jackson & Halestrap, 1996). In contrast, no inhibition by pCMBS was observed when hamster MCT2 was expressed in Sf9 insect cells (Garcia et al., 1995). MCT2, however, has, to our knowledge, not yet been studied in a native environment. It is presently unclear whether the pCMBS-insensitivity of MCT2 is maintained in the native environments of this subtype and whether the differential sensitivity to pCMBS is a discriminating feature in species other than hamster.

The purpose of the present study was to characterize and localize mechanisms for monocarboxylate transport in VDC and to identify isoforms of MCT which are present in the vestibular labyrinth. Preliminary data of this study have been presented at recent meetings (Shimozono et al., 1996, 1997).

Materials and Methods

Preparations

The method of dissection of VDC epithelium has been described earlier (Wangemann et al., 1995). Briefly, gerbils and hamsters were anesthetized with pentobarbital (50 mg/kg i.p.) and decapitated. The procedures concerning animals reported in this study were approved by the Institutional Animal Care and Use Committee at Boys Town National Research Hospital. The temporal bone containing the inner ear was removed from the gerbil and quickly transferred into cold (4°C) solution which contained (in mM): 150 Na-gluconate, 1.6 K_2HPO_4, 0.4 KH_2PO_4, 4.0 Ca-gluconate, 1.0 $MgSO_4$, 5.0 glucose for dissection. Under microscopic observation the ampullae was dissected free and a patch of epithelium including dark cell epithelium was carefully trimmed. For measurement of I_{sc} the tissue was used as a flat sheet. For the measurement of pH_i, the tissue was folded in a loop so that an optical section of VDC exclusive of the underlying connective tissue was accessible for microfluorescence measurements (Fig. 1). A rectangular aperture was used to limit the quantified fluorescence signal to that originating from VDC. For the molecular biologic studies, whole vestibular labyrinths and samples of blood were obtained from the gerbil and for the development of gene-specific primers, samples of heart, lung, liver and kidney were obtained from hamsters and gerbils.

Measurement of pH_i

pH_i was measured using the pH sensitive dye BCECF loaded into the cells as BCECF-acetoxymethylester (BCECF-AM) as described previously (Wangemann, 1996). Briefly, the folded tissue was incubated on the stage of the microscope with 10 μM BCECF-AM at room temperature for 15–20 min. Standard NaCl solution contained (in mM): 150 NaCl, 1.6 K_2HPO_4, 0.4 KH_2PO_4, 0.7 $CaCl_2$, 1.0 $MgCl_2$, 5.0 glucose. During the experiments, the tissue was continuously superfused such that the solution volume of the bath chamber was exchanged at a rate of 3 times per second. Experiments were conducted at 37°C. The preparation was alternately illuminated with light of 442 and 502 nm wavelength. The emitted light passed through a 516 nm dichroic mirror and a 531 ± 10 nm band-pass filter (Omega Optical, Brattleboro, VT). The intensity of emission in response to the two excitation wavelengths was recorded, the ratio (502/442) was computed and calibrated *vs.* pH_i at the end of each experiment.

Measurement of the Equivalent Short Circuit Current (I_{sc})

The methods were described previously (Marcus, Lin & Wangemann, 1994). Briefly, tissue was mounted in a micro-Ussing chamber by sealing the apical membrane of VDC to the aperture (80 μm diameter). The apical and basolateral sides of tissue were perfused separately and exchange of solution on each side was complete within 1 sec. Transepithelial voltage (V_t) was measured with calomel electrodes connected to the chambers via 1 M KCl brides. Transepithelial resistance (R_t) was obtained from the voltage changes induced by current pulses (50 nA for 34 msec at 0.3 Hz). Sample and hold circuitry was used to obtain a signal proportional to R_t. The equivalent short circuit current (I_{sc}) was obtained according to Ohm's law ($I_{sc} = V_t/R_t$) from measurements of V_t and R_t.

Extraction of Total RNA

Total RNA was extracted from samples of gerbil vestibular labyrinth and gerbil blood and from hamster and gerbil heart, lung, liver and

kidney. Methods employed for the extraction of RNA from vestibular labyrinth and blood were different from those employed for the large organs due to the lower amount of RNA available. Heart, lung, liver and kidney were sliced with razor blades and frozen in liquid nitrogen within 5 min of sacrifice. The frozen tissue samples were pulverized in liquid nitrogen and immediately transferred into the RNA extraction medium (TRIzol, GIBCO BRL, Life Technologies), a monophasic solution of phenol and guanidine isothiocyanate. Vestibular labyrinths from gerbils were isolated by microdissection and tissues were directly transferred from the 7°C dissection medium into TRIzol reagent within 7 min (first ear) and 15 min (second ear) of sacrifice of each animal. Tissues from 8 ears were pooled in the TRIzol reagent and disrupted by one freezing/thawing cycle. Further, gerbil blood was mixed with the TRIzol reagent. The total RNA was then extracted using TRIzol reagent according to manufacturer's procedure, was precipitated by isopropanol, and dissolved in RNase-free water (diethylpyrocarbonate treated water). The nucleic acid concentration was determined spectrophotometrically and adjusted to be between 1.0 and 2.0 μg/μl for RNA samples obtained from the large organs and to 0.3 μg/μl for RNA obtained from gerbil vestibular labyrinth and blood. The yield of RNA from the vestibular labyrinth obtained from four gerbils averaged 3 μg. RNA samples were stored at −70°C. The quality of the RNA samples from the large organs was evaluated after horizontal agarose gel electrophoresis by analyzing the presence of the 28S and 18S ribosomal RNA (*data not shown*). The quality of the small amounts of RNA extracted from the microdissected vestibular labyrinth was assessed by determining the presence of β-actin transcripts by RT-PCR (*see results*).

Before analysis of the RNA samples by reverse-transcription polymerase chain reaction (RT-PCR), DNA contamination of the RNA samples was removed by treatment with DNase I. RNA samples obtained from the large organs were treated at 37°C for 30 min with DNase I (GIBCO BRL, Life Technologies) in the presence of RNasin (Promega). Total RNA was then precipitated with ethanol in the presence of 2 M NH_4OAC. RNA samples obtained from the vestibular labyrinth or blood was treated at room temperature for 15 min with amplification-grade RNase-free DNase I (GIBCO BRL, Life Technologies) followed by heat inactivation in the presence of EDTA, according to the protocol specified by the manufacturers.

cDNA Synthesis and PCR Amplification

Total RNA was reverse transcribed into cDNA in a 20 μl reaction. The reaction contained 0.5–1.0 μg total RNA, 20 units RNasin (Promega), 1 mM dNTP (GIBCO BRL, Life Technologies), 50 units Moloney Murine Leukemia Virus Reverse Transcriptase (Perkin-Elmer, Inc.), 2.5 mM $MgCl_2$ (GIBCO BRL, Life Technologies), either 25 pmol antisense gene specific primer for MCT1 or MCT2 or 25 pmol oligo $d(T)_{17}$, 20 mM Tris-HCl and 50 mM KCl. Tris-HCl and KCl were added from a 10X PCR buffer (GIBCO BRL, Life Technologies). The RT reaction was incubated at 42°C for 50 min, 5 min at 99°C, and 5 min at 5°C.

PCR amplification was conducted in a 100 μl reaction which contained the 20 μl RT reaction mix in addition to 25 pmol each of antisense and sense primers for MCT1 or MCT2 and 2.5 units Taq DNA polymerase (GIBCO BRL, Life Technologies). The final concentrations of $MgCl_2$, KCl and Tris-HCl were adjusted to 2.5, 50 and 20 mM, respectively. The PCR reaction mix was incubated as follows: 1 denaturation cycle for 3 min at 95°C; 45 amplification cycles consisting of: denaturation for 1 min at 95°C, annealing for 1 min at 50°C and extension for 1 min at 72°C; and one extension cycle for 5 min at 72°C on a Perkin Elmer DNA Thermal Cycler 480.

The primers used for β-actin (Feve et al., 1994), MCT1 and MCT2 are shown in Table 1. Sense and antisense gene specific primers for MCT1 and MCT2 were designed based on the published sequences (GenBank/EMBL database) using the software Prime, (Wisconsin Package, Genetics Computer Group). The specificity of the primers was validated by RT-PCR of RNA obtained from hamster heart and lung known to contain MCT1 and from hamster liver and kidney known to contain MCT2 (Garcia et al., 1995) (*data not shown*). Cross-reactivity of the primers with RNA obtained from gerbil was verified by RT-PCR of RNA obtained from gerbil heart and lung (for MCT1) and from gerbil liver and kidney (for MCT2) (*data not shown*). PCR products were analyzed by horizontal electrophoresis in 2% agarose gels and visualized by ethidium bromide staining.

Table 1. PCR primers and expected PCR product sizes

Isoform	Primer sequence 5′-3′	Size
β-actin	(s)GAGACCTTCAACACCCC (a)GTGGTGGTGAAGCTGTAGCC	236 bp
MCT1	(s)TCCAGTGAGAAGTCAGCCTTCCTC (a)CTGGGGACCAACAAGGTCCATCAA	274 bp
MCT2	(s)GCAGCTTTATTGCTGTCTGTGATG (a)AGGTCCAACAAGGTCCATGAGAGT	260 bp

(s) sence primer, (a) antisence primer

Cloning and Sequencing of Amplified cDNA Fragments

Amplified cDNA fragments were extracted from the agarose gels using the QIA quick gel extraction kit (Qiagen) and cloned into a pCR®2.1 vector with a TA cloning® kit (Invitrogen). Recombinant plasmids were isolated from the colonies using the standard alkaline lysis procedure, purified by phenol/chloroform extraction, and precipitated and washed with ethanol. Insertion of the PCR product into the plasmid was confirmed by restriction endonuclease digestion with *EcoRI* and subsequent horizontal gel electrophoresis. The recombinant double stranded plasmid served as a template for cycle sequencing using M13 forward and reverse primers and fluorescence-based dideoxy nucleotides (PRISM Ready Reaction Dye Deoxy Terminator Cycle Sequencing Kit, Perkin Elmer). The sequence was then determined using the ABI Model 373 DNA Sequencer (Applied Biosystems) and confirmed by the cloning and sequencing of RT-PCR products from at least three separate RT-PCR reactions. The identity of the gerbil sequences was determined by a FastA (Wisconsin Package, Genetics Computer Group) comparison to the known GenBank/EMBL hamster sequences.

Statistics

Data of functional studies are presented as the mean ± SEM. The number of observations (n) is number of tissues. Student's t-test of paired samples was applied and a level of $P < 0.05$ was considered statistically significant.

Results

Effect of Monocarboxylates on pH_i in the Presence of CHC

Uptake of weak acids such as mono- or dicarboxylates cause acidification of pH_i if the carboxylate anion is

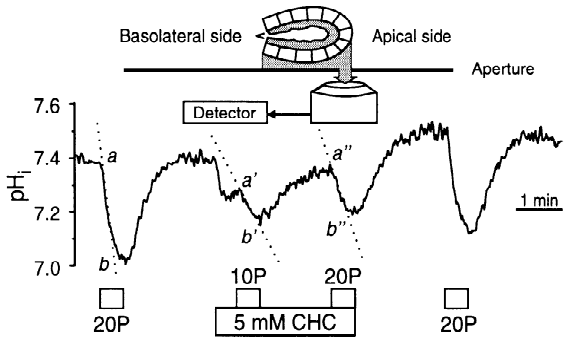

Fig. 1. Effect of pyruvate in the absence and presence of α-cyano-4-hydroxycinnamate (CHC) on cytosolic pH (pH_i) of in vestibular dark cells (VDC). The initial rates of acidification (a–b, a′–b′ and a″–b″) were obtained by linear regression (dotted lines) of the initial 3–5s quasi-linear portion of the pH_i change which occurred within 15 sec after addition of 10 mM (10P) and 20 mM pyruvate (20P). *Insert:* Diagram of the technique for the measurement of the pH_i in VDC. The tissue was folded in a loop so that an optical section was accessible for the measurement of pH_i. A rectangular aperture was used to limit the fluorescence signal to that originating mostly from VDC.

taken up together with an acid equivalent. Uptake of monocarboxylates together with an acid equivalent could occur by non-ionic diffusion of the undissociated acids or could be mediated by a transporter such as MCT or anion exchange proteins. Uptake of monocarboxylates via MCT or anion exchange proteins is expected to be blocked by CHC whereas non-ionic diffusion would not be expected to be sensitive to CHC (Halestrap, 1976; Poole & Halestrap, 1993). In a first series of paired experiments, the effect of 20 mM monocarboxylates in the absence and presence of 5 mM CHC was determined. Monocarboxylates caused an acidification of the cytosolic pH. The initial rate of this acidification was significantly reduced by CHC. Indeed, CHC reduced the initial rate of acidification induced by pyruvate from $(-27.4 \pm 2.4) \times 10^{-3}$ (Fig. 1, *a–b*) to $(-15.5 \pm 1.0) \times 10^{-3}$ pH-units/s (Fig. 1, a″–b″, $n = 5$), acetate from $(-39.6 \pm 4.6) \times 10^{-3}$ to $(-21.7 \pm 2.4) \times 10^{-3}$ pH-units/s ($n = 5$), L-lactate from $(-31.2 \pm 2.1) \times 10^{-3}$ to $(-11.0 \pm 0.5) \times 10^{-3}$ pH-units/s ($n = 5$) and *D*-lactate from $(-16.0 \pm 2.5) \times 10^{-3}$ to $(-4.5 \pm 0.7) \times 10^{-3}$ pH-units/s ($n = 5$). These observations suggest that uptake of monocarboxylates occurs via a transporter rather than solely via non-ionic diffusion.

Effect of Mono- and Dicarboxylates on pH_i

Uptake of monocarboxylates together with an acid equivalent could occur via MCT or anion exchange proteins. Anion exchange proteins transport mono- as well as dicarboxylates whereas MCT transport only monocarboxylates. Thus, the substrate specifically provides a means to distinguish between these two transport mechanisms. In a second series of experiments, the effects of the monocarboxylates pyruvate, acetate, L-lactate and D-lactate (each 20 mM) and the dicarboxylate malonate (20 mM) on pH_i of VDC were determined. The application of pyruvate, acetate, L-lactate and D-lactate induced within 5 sec a significant acidification of VDC from pH 7.30 ± 0.02 to pH 7.10 ± 0.02 ($n = 5$), pH 7.20 ± 0.05 to pH 6.87 ± 0.07 ($n = 5$), pH 7.21 ± 0.04 to pH 7.02 ± 0.03 ($n = 5$) and pH 7.34 ± 0.02 to pH 7.21 ± 0.04 ($n = 5$), respectively. In contrast, the application of malonate caused within 15 sec no significant effect on pH_i (pH 7.30 ± 0.06 *vs.* pH 7.32 ± 0.07; $n = 3$). These observations demonstrate that monocarboxylates but not dicarboxylates are taken up by VDC together with an acid equivalent. Further, these observations suggest that monocarboxylates are taken up via MCT rather than anion exchange proteins.

Effect of Monocarboxylates on pH_i in the Presence of DIDS

The sensitivity to DIDS provides another means to distinguish between MCT and anion exchange proteins mediated uptake of monocarboxylates. Uptake via anion exchange proteins would be expected to be inhibited by 1 μM DIDS, a concentration which would not be expected to cause inhibition of MCT. Indeed, DIDS is known to inhibit anion exchange proteins mediated transport of monocarboxylates with a K_i of 0.04 μM and MCT mediated transport with a thousandfold higher K_i of 40 μM (Poole & Halestrap, 1993). Thus, sensitivity to 1 μM DIDS provides a means to distinguish between these two transporters. In a third series of paired experiments, the effect of 20 mM acetate in the absence and presence of 1 μM DIDS was determined. DIDS had no significant effect on the initial rate of acidification ($(-33.3 \pm 0.8) \times 10^{-3}$ *vs.* $(-32.4 \pm 0.4) \times 10^{-3}$ pH-units/s, ($n = 3$)). These observations support the conclusion that monocarboxylates are taken up by VDC via MCT rather than anion exchange proteins.

Transport Kinetics of MCT in VDC

In a fourth series of experiments, the initial acidification rates induced by different concentrations of monocarboxylates were measured to determine the transport kinetics of MCT (Poole et al., 1989, Wang et al., 1994). The initial rates of acidification induced by the monocarboxylates pyruvate, acetate, L-lactate and D-lactate in VDC were dose-dependent in the range between 1 and 20 mM (*see* example in Fig. 2*A*). Uptake of monocarboxylates saturated at the higher concentrations compared to non-ionic diffusion of the undissociated acid.

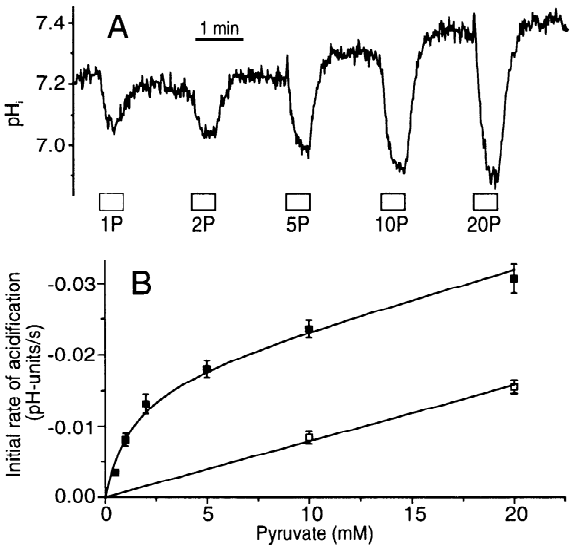

Fig. 2. Kinetics of pyruvate uptake in VDC. (*A*) pH_i changes induced by 1, 2, 5, 10 and 20 mM pyruvate (P). (*B*) The concentration dependence of the initial rate of acidification induced by pyruvate in the absence of CHC (closed symbols, *see* Fig. 2*A* for original data) and in the presence of CHC (open symbols, *see* Fig. 1 for original data). The data for pyruvate in the absence of CHC were fitted by nonlinear least squares algorithm to the Michaelis-Menten equation whereas the data for pyruvate in the presence of CHC were fitted by linear regression (*see text*).

Uptake of monocarboxylates by non-ionic diffusion was determined as CHC-insensitive portion of the cytosolic acidification (*see* example in Fig. 1). The initial rates of acidification induced by monocarboxylates in the presence of 5 mM CHC were linearly related to the monocarboxylate concentrations (*see* example in Fig. 2*B*). The slope of this linear regression (S_{lr}) was used to calculate the apparent rate of monocarboxylate uptake via non-ionic diffusion according to $V_{CHC} = S_{lr} \times [MC]$ where [MC] represents the concentration of monocarboxylates. To obtain the initial rate of acidification mediated by MCT (V_{MCT}), the initial rate of acidification in the absence of CHC (V_{total}) was subtracted by the apparent rate of monocarboxylate uptake via non-ionic diffusion (V_{CHC}) according to $V_{MCT} = V_{total} - V_{CHC}$. Values for V_{MCT} were fitted by a nonlinear least-squares algorithm to the Michaelis-Menten equation ($V_{MCT} = V_{max} \times [MC]/(K_m + [MC])$) where K_m and V_{max} have their usual meanings. K_m and V_{max} values for pyruvate, acetate, L-lactate and D-lactate are given in Table 2. For comparison, published K_m values are given for MCT in mouse Ehrlich Lettré tumor cells (Carpenter & Halestrap, 1994), rat liver cell (Jackson & Halestrap, 1996) and guinea pig heart cells (Poole et al., 1989). In VDC pyruvate had the highest affinity (lowest K_m). The affinities for the L- and D-isomer of lactate were significantly different, demonstrating that the transporter is stereoselective.

Table 2. Kinetic parameters for uptake of monocarboxylate into vestibular dark cell (VDC)

		K_m (mM)				V_{max} (10^{-3} pH-units/s)
Substrates	*n*	VDC	Liver*	Heart*	Tumor*	VDC
Pyruvate	7	1.3 ± 0.3	1.3	0.07	0.7	−17 ± 2
Acetate	9	3.7 ± 1.1	5.4	–	3.7	−17 ± 1
L-Lactate	9	3.8 ± 0.9	4.7	2.3	4.5	−20 ± 2
D-Lactate	7	7.3 ± 1.0	27.0	6.6	27.5	−16 ± 1

* Data cited from papers given in the text

Effect of Monocarboxylate in the Presence of pCMBS on pH_i

A substantial difference between MCT1 and MCT2, the differential sensitivity to pCMBS, has been observed when the isoforms were expressed in Sf9 insect cells. It is currently unclear, however, whether this discriminating feature is maintained in the native environments of the subtypes and present in species other than hamster. Nevertheless, in a fifth series of paired experiments, the effect of 5 mM acetate in the absence and presence of 500 μM pCMBS was determined. pCMBS had no significant effect on the initial rate of acetate-induced acidification ($(-12.7 \pm 1.1) \times 10^{-3}$ *vs.* $(-11.4 \pm 1.0) \times 10^{-3}$ pH-units/s; $n = 5$). These observations demonstrate that MCT in VDC is insensitive to pCMBS suggesting that MCT consists mainly of the MCT2 subtype.

Effect of Apical and Basolateral Application of Monocarboxylates on I_{sc}

K^+ secretion by VDC can be monitored by measuring I_{sc} in the micro-Ussing chamber which allows individual perfusion of the apical and basolateral membrane. Acidification of pH_i has previously been shown to cause a transient stimulation of I_{sc} (Wangemann et al., 1995). Thus, it is possible to determine whether monocarboxylates induce acidification when applied solely to the apical or basolateral membrane. In a sixth series of experiments, the effect of apical and basolateral application of the monocarboxylates pyruvate, acetate, L-lactate and D-lactate and the dicarboxylate malonate (each 5 mM) on I_{sc} were determined. Apical application of pyruvate, acetate, L-lactate and D-lactate caused transient increase of I_{sc} from 674 ± 57 to 739 ± 62 μA/cm^2 ($n = 5$; Fig. 3*A*, a–b), 653 ± 51 to 697 ± 55 ($n = 5$), 671 ± 55 to 739 ± 55 ($n = 5$) and 684 ± 56 to 721 ± 55 ($n = 5$), respec-

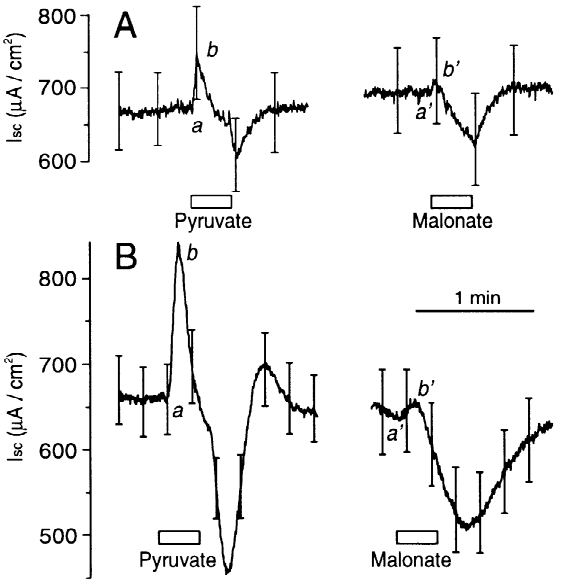

Fig. 3. Effect of apical (*A*) and basolateral (*B*) application of 20 mM pyruvate and malonate on the short circuit current (I_{sc}) of VDC. Apical and basolateral application of the monocarboxylate pyruvate caused a transient increase of I_{sc} (*a–b*) whereas the dicarboxylate malonate caused only a minimal increase in I_{sc} (a′–b′). The time-bar in *B* applies to the entire figure.

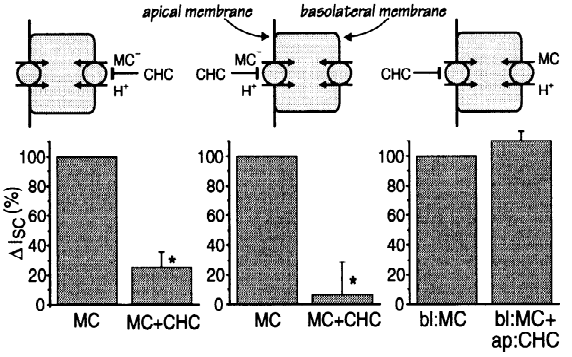

Fig. 4. Localization of MCT to the apical and basolateral membrane of VDC. The I_{sc} was measured and the monocarboxylate 5 mM acetate was applied to the apical or basolateral membrane in the absence or presence of 5 mM CHC. *Left panel:* Effect of basolateral acetate in the absence (MC) and presence of basolateral CHC (MC + CHC). *Middle panel:* Effect of apical acetate in the absence (MC) and presence of apical CHC (MC + CHC). *Right panel:* Effect of basolateral acetate in the absence (bl:MC) and presence of apical CHC (bl:MC + ap:CHC). Significant effects are marked (*).

tively. In contrast, apical application of malonate caused no significant effect on I_{sc} (694 ± 59 *vs.* 708 ± 59 μA/cm^2 (n = 5) Fig. 3*A*, a′–b′). Basolateral application of pyruvate, acetate, L-lactate and D-lactate caused transient increase of I_{sc} from 659 ± 42 to 834 ± 55 μA/cm^2 (n = 9; Fig. 3*B*, a–b), 643 ± 46 to 795 ± 56 (n = 9), 659 ± 37 to 798 ± 44 (n = 9) and 632 ± 49 to 764 ± 52 (n = 9), respectively. In contrast, basolateral application of malonate caused no significant effect on I_{sc} (637 ± 48 *vs.* 654 ± 49 μA/cm^2 (n = 9), Fig. 3*B*, a′–b′). These observations suggest that VDC take up monocarboxylates but not dicarboxylates across both the apical and basolateral membrane. From this series of experiments it remained unclear whether uptake of monocarboxylates were mediated by non-ionic diffusion or MCT.

Effect of Apical and Basolateral Application of Monocarboxylate on I_{sc} in the Presence of CHC

Monocarboxylates induced acidification when applied to the apical or basolateral membrane of VDC. If uptake of monocarboxylates were mediated by MCT, it would be expected that the observed increase in I_{sc} would be sensitive to CHC. In a seventh series of paired experiments, the effect of apical and basolateral application of 5 mM acetate was determined in the absence and presence of 5 mM CHC. Data were normalized to the effects observed in the absence of CHC (Fig. 4). In the absence of CHC, basolateral application of acetate caused an increase of I_{sc} by a factor of 1.27 ± 0.03 (n = 8; 100% in the left panel of Fig. 4). This acetate-induced increase of I_{sc} was significantly reduced to a factor of 1.11 ± 0.02 in the presence of CHC applied on the same (basolateral) side. Similarly, an increase of I_{sc} was observed when acetate was applied to the apical side of VDC. In the absence of CHC, apical application of acetate caused an increase of I_{sc} by a factor of 1.04 ± 0.01 (n = 6; 100% in the middle panel of Fig. 4). This acetate-induced increase of I_{sc} was significantly reduced to a factor of 1.001 ± 0.001 in the presence of CHC when applied on the same (apical) side. These observations would suggest that MCT is present in both, the apical and basolateral membrane of VDC unless, the effect of CHC would not be limited to the side the drug was applied. Thus, it was necessary to demonstrate that CHC applied to one side does not affect uptake of monocarboxylates across the other side of the epithelium. In the absence of CHC, basolateral application of acetate caused an increase of I_{sc} by a factor of 1.08 ± 0.01 (n = 6; 100% in the right panel of Fig. 4). This acetate-induce increase of I_{sc} remained unchanged in the presence of CHC applied to the other (apical) side (factor of 1.09 ± 0.01). These results verify that CHC did not cross over from the apical to the basolateral side and that VDC contain MCT in both the apical and basolateral membrane.

RT-PCR Amplification and Sequencing of MCT1 and MCT2

To determine which subtypes may be present in VDC, we determined the presence of transcripts for MCT1 and

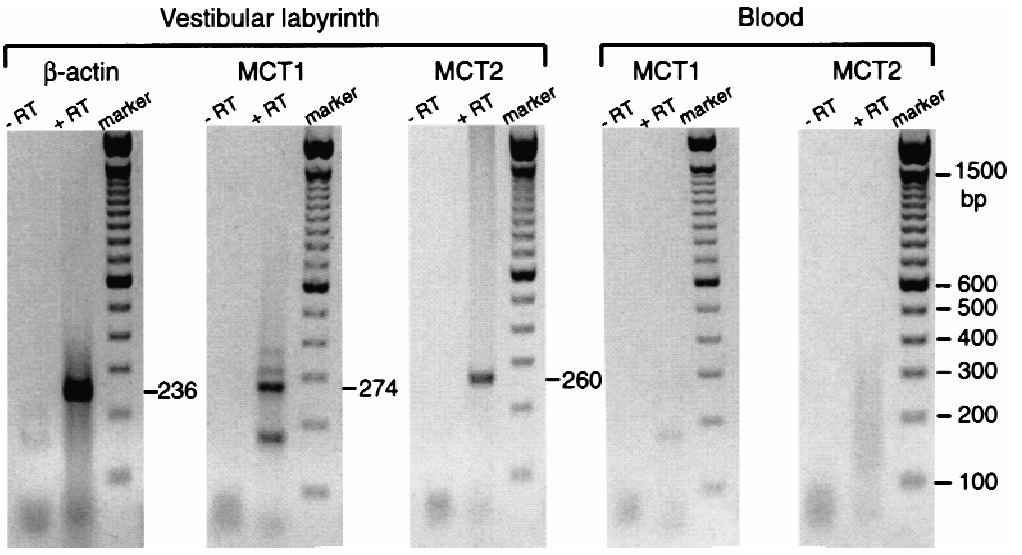

Fig. 5. Agarose gel electrophoresis of reverse-transcriptase polymerase chain reaction (RT-PCR) products. RT-PCR was performed with gene-specific primers for β-actin, MCT1 and MCT2 on total RNA extracted from gerbil vestibular labyrinth and from gerbil blood. RT-PCR products of the expected size obtained in reactions in which reverse-transcriptase was present (lanes labeled '+RT') suggest the presence of the respective transcript. Absence of RT-PCR products in reactions in which reverse-transcriptase was absence (lanes labeled '-RT') demonstrate that the RNA sample was free of DNA contamination. RT-PCR products that were less than 100 bp in size presumably represent the formation of primer-dimers between the primer pairs. The DNA size marker consisted of 15 blunt-ended fragment between 100 and 1500 bp in multiples of 100 bp.

MCT2 in the vestibular labyrinth by RT-PCR. The presence of transcripts was determined in RNA obtained from the vestibular labyrinth rather than from VDC because VDC cannot readily be isolated from the vestibular labyrinth. The quality of the small quantities of RNA obtained from vestibular labyrinth was assessed by RT-PCR of β-actin (Fig. 5). Agarose gel electrophoresis revealed a PCR product of the predicted size, 236 bp (Fig. 5). This observation demonstrates that total RNA extracted from vestibular labyrinth was intact. RT-PCR performed with gene-specific MCT1 and MCT2 primer pairs on total RNA extracted from vestibular labyrinth revealed PCR products of the expected sizes of 274 and 260 bp, respectively (Fig. 5). The nucleotide sequences of the amplified fragments of MCT1 and MCT2 from gerbil vestibular labyrinth have been deposited to genebank under the accession number AF029766 and AF029767, respectively. Comparison of these sequences to known sequences verified that they are fragments of MCT1 and MCT2 (*see* Discussion). These observations demonstrate that vestibular labyrinth contains transcripts for both, MCT1 and MCT2.

It is conceivable that blood present inside the capillaries of the microdissected vestibular labyrinth provided a source of mRNA for the MCT subtypes. To evaluate this possibility, we determined whether transcripts for MCT1 and MCT2 can be amplified from total RNA extracted from blood. Agarose gel electrophoresis of PCR products revealed that neither the primers for MCT1 nor those of MCT2 amplified a transcript (Fig. 5). These observations demonstrate that blood contaminating our samples of vestibular labyrinth did not provide a source of message for either MCT subtype.

Discussion

Evidence for MCT in VDC on Both Apical and Basolateral Sides

Several lines of evidence suggest that VDC contain MCT: Uptake of the monocarboxylate anion together with an acid equivalent caused acidification of pH_i which was sensitive to CHC, suggesting that uptake was mediated by a transporter rather than solely by non-ionic diffusion (Fig. 1). Non-ionic diffusion of the undissociated acid, however, may in part be responsible for the uptake of monocarboxylates because the undissociated pyruvic acid (pK_a 2.5), acetic acid (pK_a 4.8), L- and D-lactic acid (pK_a 3.9) are highly lipid soluble and equilibrate readily across cell membranes (Walter & Gutknecht, 1984). Evidence suggesting that monocarboxylates are taken up via MCT rather than via anion exchange proteins comes from the observations that monocarboxylates caused acidification of pH_i but that the dicarboxylate malonate did not, that monocarboxylate-induced acidification was not inhibited by 1 μM DIDS and that the K_m for L-lactate (3.8 mM) was about half than that for D-lactate (7.3 mM) while V_{max} were similar for both isomers (Table 2).

MCT in VDC was characterized by determining the sensitivity to pCMBS. MCT was found to be insensitive to pCMBS suggesting that MCT in VDC consisted mainly of MCT2 (*see* Introduction). This conclusion, however, is weakened by the fact that it is unclear whether the differential sensitivity to pCMBS is a feature particular to the hamster MCT subtypes or the insect cell expression system.

Evidence for the presence of MCT in both the apical and basolateral membrane of VDC was obtained from measurement of I_{sc} (Fig. 3). I_{sc} is a measure for K^+ secretion which has been shown to be sensitive to pH_i (Wangemann et al., 1995). Indeed, effects induced by pyruvate, acetate, L- and D-lactate on I_{sc} and pH_i observed in the present study are qualitatively similar to the effects induced by the monocarboxylate propionate observed in a previous study (Wangemann et al., 1995).

Evidence for MCT1 and MCT2 in the Vestibular Labyrinth

Since the MCT subtypes MCT1 and MCT2 cannot readily be distinguished in functional studies, we determined the presence of their transcripts. The presence of transcripts was determined in RNA extracted from vestibular labyrinth which contains VDC (Fig. 5). For technical reasons, RNA was extracted from vestibular labyrinth rather than from VDC directly. Thus, it remains unclear whether transcripts were present in VDC and/or in another cell type present in vestibular labyrinth. Blood inside the capillary bed within vestibular labyrinth, however, was ruled out as a source of transcripts for MCT1 and MCT2 (Fig. 5).

The identity of the amplified transcripts was determined by sequencing and comparison to known sequences. The 228 bp fragment of gerbil vestibular labyrinth MCT1 and the 213 bp fragment of gerbil vestibular labyrinth MCT2 had a 95.6% nucleotide sequence identity with the MCT1 cDNA from hamster CHO cells and a 87.3% nucleotide sequence identity with the MCT2 cDNA from Syrian hamster liver, respectively (Garcia et al., 1994*b*, 1995). Nucleotide sequence homologies between the gerbil sequence fragments and known sequences are summarized in Table 3. The putative amino acid sequence of the gerbil vestibular labyrinth MCT1 had a 98.7% identity in 75 amino acids with the hamster CHO cells MCT1 and the putative amino acid sequence of the gerbil vestibular labyrinth MCT2 had a 83.1% identity in 71 amino acids with the Syrian hamster liver MCT2. These results indicate that both primers amplified sequences unique for MCT1 and MCT2. It remains to be determined which transcripts present in the vestibular labyrinth are present in VDC and whether these transcripts are expressed into functional proteins. The latter aspect is of special importance since it has been shown that the correlation between MCT transcripts and proteins is poor (Jackson et al., 1997).

Table 3. Nucleotide sequence homologies

	Accession numbers	MCT1 gerbil
MCT1 hamster	L25842	95.6% in 228 nt
MCT1 mouse	X82438	93.4% in 228 nt
MCT1 rat	X86216	88.6% in 228 nt
MCT1 human	L31801	85.0% in 228 nt
MCT2 hamster	L31957	61.8% in 228 nt
MCT3 rat	U87627	65.8% in 38 nt
MCT3 human	U81800	58.9% in 56 nt
	Accession numbers	**MCT2 gerbil**
MCT2 hamster	L31957	87.3% in 213 nt
MCT2 rat	X97445	83.1% in 213 nt
MCT1 hamster	L25842	61.4% in 215 nt
MCT3 rat	U87627	57.5% in 174 nt
MCT3 human	U81800	54.6% in 174 nt

Physiological Relevance of MCT in VDC

The present study provides the first description of a transport mechanism for the uptake of glycolytic substrates into VDC. Although GLUT1 has been identified immunohistochemically in other parts of the inner ear including microvascular endothelial cells and strial basal cells of the cochlea, GLUT1 has been shown to be absent from strial marginal cells (Ito, Spicer & Schulte, 1993) which are the cochlear equivalent to VDC (Wangemann, 1995). Glucose may be the substrate of highest physiological relevance, however, the uptake of lactate and pyruvate may be of importance under aerobic conditions as well as under ischemic and hypoxic conditions. Uptake of glycolytic substrates may be of special importance for VDC since immunohistochemical and ultrastructural evidence suggests that at least rat VDC do not have gap junctions, which would allow the exchange of a variety of small molecules (Kikuchi et al., 1995). Thus, individual VDC cannot rely on adjacent cells for the acquisition of glycolytic substrates but must themselves take up these substrates from their environment which is endolymph on the apical side and perilymph on the basolateral side (Wangemann & Schacht, 1996). Whether endolymph, like perilymph, provides a reservoir for glycolytic substrates is currently unclear. Neither the lactate nor the pyruvate concentration in endolymph has been determined to our knowledge. Whether and how the monocarboxylates pyruvate and lactate enter perilymph is currently unclear.

The uptake of monocarboxylates into VDC may be necessary to meet the metabolic fuel requirements of

VDC. Support for the hypothesis that lactate and pyruvate can be used as metabolic fuel in VDC comes from the finding that lactate and pyruvate are sufficient to maintain the endocochlear potential (Kambayashi et al., 1982) which is dependent on K^+ secretion by strial marginal cells (Wangemann, 1995).

Whether MCT in VDC supports monocarboxylate uptake or export is currently unclear, since it is unknown which direction of transport is supported by the present monocarboxylate$^-$ and H^+ gradients. Estimations of the gradients, however, are consistent with the hypothesis that MCT supports uptake of the monocarboxylates lactate and pyruvate. The intracellular concentrations of lactate and pyruvate in VDC are unknown but may be similar to those in liver cells. Both the liver and the vestibular labyrinth contain a high activity of LDH5 (Lotz & Kuhl, 1968). Unlike other subtypes of LDH, LDH5 favors the conversion of lactate into pyruvate (Cahn et al., 1962). Therefore, we based our estimation of the lactate and pyruvate concentrations in VDC on observations made in liver cells. Based on measurements in liver cells (Greenbaum, Gumaa & Mclean, 1971), the lactate and pyruvate concentrations in VDC can be estimated to be 1.7 and 0.1 mM, respectively. The extracellular concentrations in endolymph may be similar to perilymph which has been found to contain 3.9–4.5 mM lactate and 0.3 mM pyruvate (Thalmann, Myoshi & Thalmann, 1972; Scheibe & Haupt, 1985). The resulting gradients for lactate (1.7 *vs.* 3.9–4.5 mM) and pyruvate (0.1 *vs.* 0.3 mM) would support uptake of these monocarboxylates into VDC assuming a transmembrane pH-gradient of about 0.2 pH-units. Further studies are needed to verify these estimates. Further, it would be of interest to determine which subtype of MCT is expressed in VDC.

This work was supported by Research Grant Number R01-DC-01098 from the National Institute on Deafness and Other Communication Disorders, National Institutes of Health.

References

Cahn, R.D., Kaplan, N.O., Levine, L., Zwilling, E. 1962. Nature and development of lactic dehydrogenases. *Science* **136:**962

Carpenter, L., Halestrap, A.P. 1994. The kinetics, substrate and inhibitor specificity of the lactate transporter of Ehrlich-Lettre tumor cells studied with the intracellular pH indicator BCECF. *Biochem J.* **304:**751–761

Carpenter, L., Poole, R.C., Halestrap, A.P. 1996. Cloning and sequencing of the monocarboxylate transporter from mouse Ehrlich-Lettre tumor cell confirms its identity as MCT1 and demonstrates that glycosylation is not required for MCT1 function. *Biochim. Biophys. Acta* **1279:**157–163

Deuticke, B., Rickert, I., Beyer, E. 1978. Stereoselective, SH-dependent transfer of lactate in human erythrocyte. *Biochim. Biophys. Acta* **507:**137–155

Edlund, G.L., Halestrap, A.P. 1988. The kinetics of transport of lactate and pyruvate into rat hepatocytes. Evidence for the presence of a specific carrier similar to that in erythrocytes. *Biochem. J.* **249:**117–126

Feve, B., Elhadri, K., Quignard-Boulange, A., Pairault, J. 1994. Transcriptional down-regulation by insulin of the β_3-adrenergic receptor expression in 3T3-F442A adipocytes: A mechanism for repressing the cAMP signaling pathway. *Proc. Natl. Acad. Sci. USA* **91:**5677–5681

Garcia, C.K., Li, X., Luna, J., Francke, U. 1994*a*. cDNA cloning of the human monocarboxylate transporter 1 and chromosomal localization of the SLC16A1 locus to 1p13.2-p12. *Genomics* **23:**500–503

Garcia, C.K., Goldstein, J.L., Pathak, R.K., Anderson, R.G.W., Brown, M.S. 1994*b*. Molecular characterization of a membrane transporter for lactate, pyruvate, and other monocarboxylates: implications for the Cori cycle. *Cell* **76:**858–873

Garcia, C.K., Brown, M.S., Pathak, R.K., Goldstein, J.L. 1995. cDNA cloning of MCT2, a second monocarboxylate transporter expressed in different cells than MCT1. *J. Biol. Chem.* **270:**1843–1849

Greenbaum, A.L., Gumaa, K.A., Mclean, P. 1971. The distribution of hepatic metabolites and the control of the pathways of carbohydrate metabolism in animals of different dietary and hormonal status. *Biochem. Biophys.* **143:**617–663

Halestrap, A.P. 1976. Transport of lactate and pyruvate into human erythrocytes. *Biochem. J.* **156:**193–207

Ito, M., Spicer, S.S., Schulte, B.A. 1993. Immunohistochemical localization of brain type glucose transporter in mammalian inner ears: Comparison of developmental and adult stage. *Hear. Res.* **71:**230–238

Jackson, V.N., Price, N.T., Halestrap, A.P. 1995. cDNA cloning of MCT1, a monocarboxylate transporter from rat skeletal muscle. *Biochim. Biophys. Acta* **1238:**193–196

Jackson, V.N., Halestrap, A.P. 1996. The kinetics, substrate, and inhibitor specificity of the monocarboxylate (Lactate) transporter of rat liver cells determined using the fluorescent intracellular pH indicator, 2′, 7′-bis(carboxyethyl)-5(6)-carboxyfluorescein. *J. Biol. Chem.* **271:**861–868

Jackson, V.N., Price, N.T., Carpenter, L., Halestrap, A.P. 1997. Cloning of monocarboxylate transporter isoform MCT2 from rat testis provides evidence that expression in tissues is species-specific and may involve post-transcriptional regulation. *Biochem. J.* **324:**447–453

Kambayashi, J., Kobayashi, T., Marcus, N.Y., DeMott, J.E., Thalmann, I., Thalmann, R. 1982. Minimal concentrations of metabolic substrates capable of supporting cochlear potentials. *Hear. Res.* **7:**105–114

Kikuchi, T., Kimura, R.S., Paul, D.L., Adams, J.C. 1995. Gap junctions in the rat cochlea: immunohistochemical and ultrastructural analysis. *Anat. Embryol.* **191:**101–118

Lotz, P., Kuhl, K.D. 1968. Die Lactatdehydrogenase des Innenohres. Archiv. klin. exp. Ohr.-Nas. Kehlk. Heilk. **192:**237–248

Marcus, D.C., Liu, J., Wangemann, P. 1994. Transepithelial voltage and resistance of vestibular dark cell epithelium from the gerbil ampulla. *Hear. Res.* **73:**101–108

Poole, R.C., Halestrap, A.P., Price, S.J., Levi, A.J. 1989. The kinetics of transport of lactate and pyruvate into isolated cardiac myocytes from guinea pig. Kinetic evidence for the presence of a carrier distinct from that in erythrocytes and hepatocytes. *Biochem. J.* **264:**409–418

Poole, R.C., Halestrap, A.P. 1993. Transport of lactate and other monocarboxylates across mammalian plasma membranes. *Am. J. Physiol.* **264:**C761–C782

Scheibe, F., Haupt, H. 1985. Biochemical differences between peri-

lymph, cerebrospinal fluid and blood plasma in the guinea pig. *Hear. Res.* **17:**61–66

Shimozono, M., Liu, J., Wangemann, P. 1996. Vestibular dark cells contain a H^+/monocarboxylate$^-$ cotransporter in their basolateral membrane. *J. Gen. Physiol.* **108:**18*a* (*abstr.*)

Shimozono, M., Liu, J., Wangemann, P. 1997. Vestibular dark cells and strial marginal cells contain a H/monocarboxylate cotransporter *Assoc. Res. Otolaryngol.* **20:**172 (*Abstr.*)

Thalmann, R., Miyoshi, T., Thalmann, I. 1972. The influence of ischemia upon energy reserves of inner ear tissues. *Laryngoscope* **82:**2249–2272

Walter, A., Gutknecht, J. 1984. Monocarboxylic acid permeation through lipid bilayer membranes. *J. Membrane Biol.* **77:**255–264

Wang, X., Levi, A.J., Halestrap, A.P. 1994. Kinetics of the sarcolemmal lactate carrier in single heart cells using BCECF to measure pH_i. *Am. J. Physiol.* **267:***H*1759–*H*1769

Wangemann, P., Liu, J., Marcus, D.C. 1995. Ion transport mechanisms responsible for K^+ secretion and the transepithelial voltage across marginal cells of stria vascularis in vitro. *Hear. Res.* **84:**19–20

Wangemann, P., Liu, J., Shiga, N. 1995. The pH-sensitivity of transepithelial K^+ transport in vestibular dark cells. *J. Membrane Biol.* **147:**255–262

Wangemann, P. 1995. Comparison of ion transport mechanisms between vestibular dark cells and strial marginal cells. *Hear. Res.* **90:**149–157

Wangemann, P., Liu, J., Shiga, N. 1996 Vestibular dark cells contain the Na^+/H^+ exchanger NHE-1 in the basolateral membrane. *Hear. Res.* **94:**94–106

Wangemann, P., Schacht, J. 1996 Cochlear homeostasis. *In:* Springer Handbook of Auditory Research: The Cochlea. P. Dallos, A.N. Popper, R. Fay, editors. pp. 130–185

Yoon, H., Fanelli, A., Grollman, E.F., Philp, N. 1997 Identification of a unique monocarboxylate transporter (MCT3) in retinal pigment epithelium. *Biochem. Biophys. Res. Commun.* **234:**90–94